

# Analysis of building deformation in landslide area using multisensor PSInSAR<sup>TM</sup> technique



Andrea Ciampalini\*, Federica Bardi, Silvia Bianchini, William Frodella, Chiara Del Ventisette, Sandro Moretti, Nicola Casagli

Department of Earth Sciences, University of Firenze, Via La Pira 4, 50121 Firenze, Italy

## ARTICLE INFO

### Article history:

Received 25 March 2014

Accepted 23 May 2014

### Keywords:

Landslide

Radar

PSInSAR

Buildings

Damages

## ABSTRACT

Buildings are sensitive to movements caused by ground deformation. The mapping both of spatial and temporal distribution, and of the degree of building damages represents a useful tool in order to understand the landslide evolution, magnitude and stress distribution. The high spatial resolution of space-borne SAR interferometry can be used to monitor displacements related to building deformations. In particular, PSInSAR technique is used to map and monitor ground deformation with millimeter accuracy. The usefulness of the above mentioned methods was evaluated in San Fratello municipality (Sicily, Italy), which was historically affected by landslides: the most recent one occurred on 14th February 2010. PSInSAR data collected by ERS 1/2, ENVISAT, RADARSAT-1 were used to study the building deformation velocities before the 2010 landslide. The X-band sensors COSMO-SkyMed and TerraSAR-X were used in order to monitor the building deformation after this event. During 2013, after accurate field inspection on buildings and structures, damage assessment map of San Fratello were created and then compared to the building deformation velocity maps. The most interesting results were obtained by the comparison between the building deformation velocity map obtained through COSMO-SkyMed and the damage assessment map. This approach can be profitably used by local and Civil Protection Authorities to manage the post-event phase and evaluate the residual risks.

© 2014 The Authors. Published by Elsevier B.V. This is an open access article under the CC BY-NC-ND license (<http://creativecommons.org/licenses/by-nc-nd/3.0/>).

## Introduction

Landslides are globally widespread phenomena, causing a significant number of human loss of life and injury, as well as extensive economic damages to private and public properties. In Europe and in Italy in particular, where half a million active landslides exist, mass movements represent the primary cause of death caused by natural hazards (Guzzetti et al., 1999, 2012). Recently, significant results in the study of ground deformation were obtained using spaceborne Synthetic Aperture Radar (SAR) sensors, locally integrated with ground observations (Ferretti et al., 2001; Guzzetti et al., 2009; Lauknes et al., 2010; Herrera et al., 2010, 2013; Tomás et al., 2012). This approach allows delivering innovative and accurate information relevant to the Civil Defense Authorities covering the pre-event, event and post-event management phases. Nowadays slow ground deformations can be easily detected and monitored using satellite radar techniques at a relatively low

cost. C-band satellites acquire SAR images since 1992, providing a very wide archive of the ground displacements historical evolution of a selected area. These sensors are characterized by a medium spatial resolution (20 m × 4 m) and a 35 days revisiting time. The new X-band COSMO-SkyMed (CSK) and TerraSAR-X (TSX) missions reduced the revisiting time to 4 (CSK) and 11 (TSX) days, enhancing the spatial resolution to 1 m × 1 m. Classical Differential Interferometry (DInSAR) is used to measure the relative motion between two image acquisitions (Costantini et al., 2000; Crosetto et al., 2011). A phase difference image or interferogram, which is directly connected to ground motion, can be obtained. PSInSAR is a non-invasive surveying technique used to calculate motions of individual ground and structure point-like target over wide-areas (Ferretti et al., 2000). The PSI technique takes conventional DInSAR a step further by correcting the atmospheric, orbital and DEM errors in order to derive relatively precise displacement and velocity measurements at specific points on the ground. This well-established technique is particularly useful in landslides mapping and monitoring (Liu et al., 2013; Bianchini et al., 2014a). San Fratello is a town located in the Messina Province (Sicily, Italy), which was affected in the last three centuries by at least three important landslides: the first two, occurred in 1754 and 1922 respectively,

\* Corresponding author. Tel.: +39 0552757785.

E-mail addresses: [andrea.ciampalini@unifi.it](mailto:andrea.ciampalini@unifi.it), [andrea.ciampalini76@gmail.com](mailto:andrea.ciampalini76@gmail.com) (A. Ciampalini).

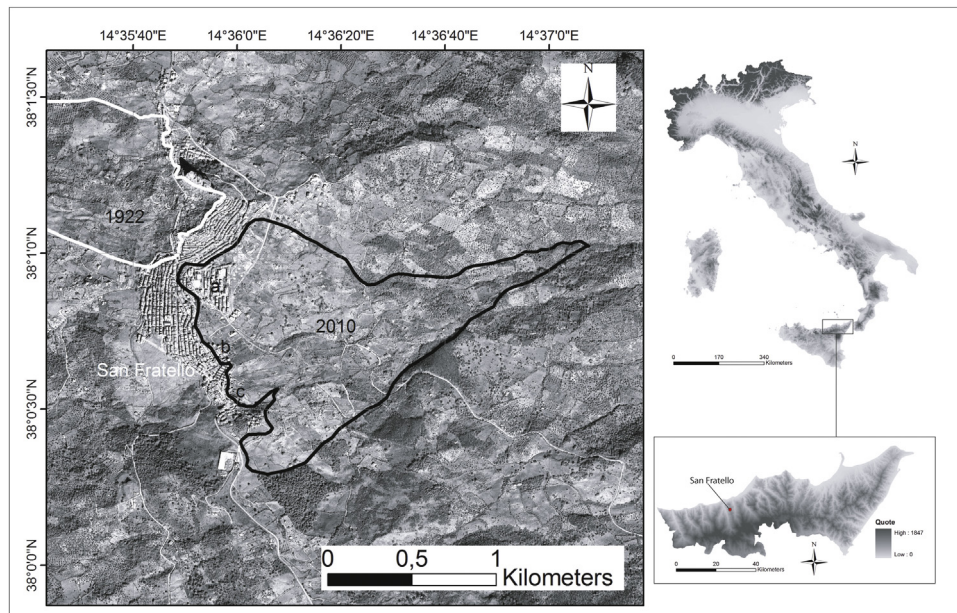


**Fig. 1.** Location of the study area and 1922 and 2010 landslides boundaries. (a) Stazzone quarter; (b) Riana quarter; (c) San Benedetto quarter.

destroyed the northern sector of the town, while the most recent one took place on the 14th February 2010, affecting the mid-eastern quarters of the town. This latter landslide, which is still active, caused severe damages to buildings and infrastructures with an estimated cost of 300 million Euros for the disaster mitigation and reconstruction program. This work presents an analysis of the San Fratello town building deformation velocities, obtained by the combined of PSI data and buildings map, with the aim of understanding the deformation evolution of the involved structures. In particular, C-band data collected before the 2010 event, were used to evaluate the presence of precursory symptoms of instability, whereas the X-band data, collected after the event, were analyzed in order to detect the residual risks in the post-event phase. Finally, the obtained post-event building deformation velocity map was

compared with the damage assessment map. This application, based on the PSInSAR technique, can be suitable to evaluate how the abundance of the elements at risk in a landslide affected area may change with time, contributing to the risk assessment, which is very important for decision making by Civil Protection Authorities, especially during the landslide post-event phase.

### Geological setting

The town of San Fratello is located in the northeastern sector of Sicily (Italy), along the Tyrrhenian coastline (Fig. 1), close to the boundary between the Nebrodi and Peloritani mountain chains. The study area was historically affected by landslides (Goswami et al., 2011; Mondini et al., 2011; Del Ventisette et al., 2012;

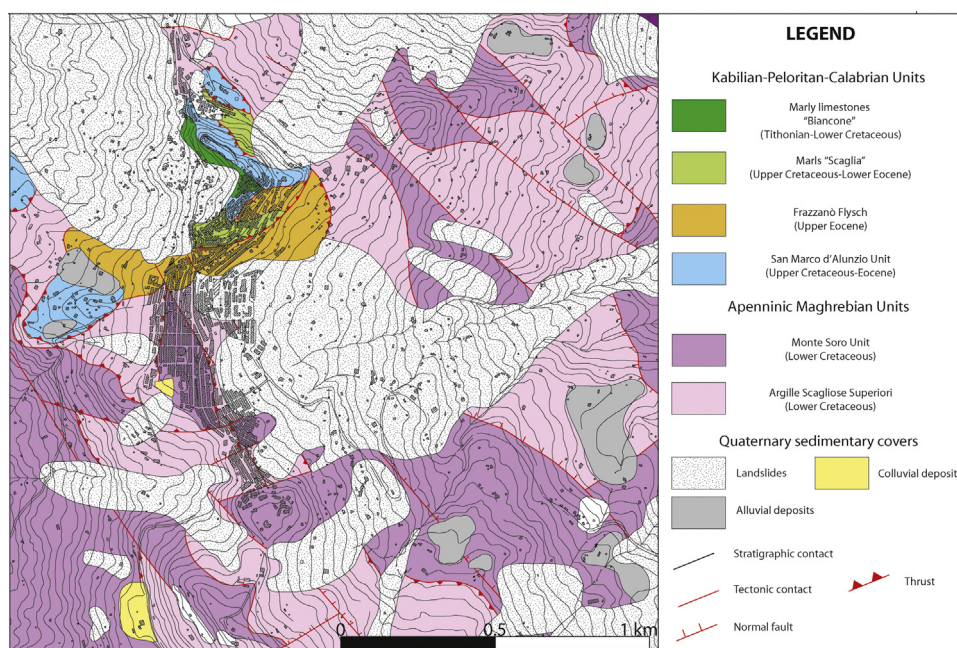


**Fig. 2.** Schematic geological map of the town of San Fratello (courtesy of DRPC).



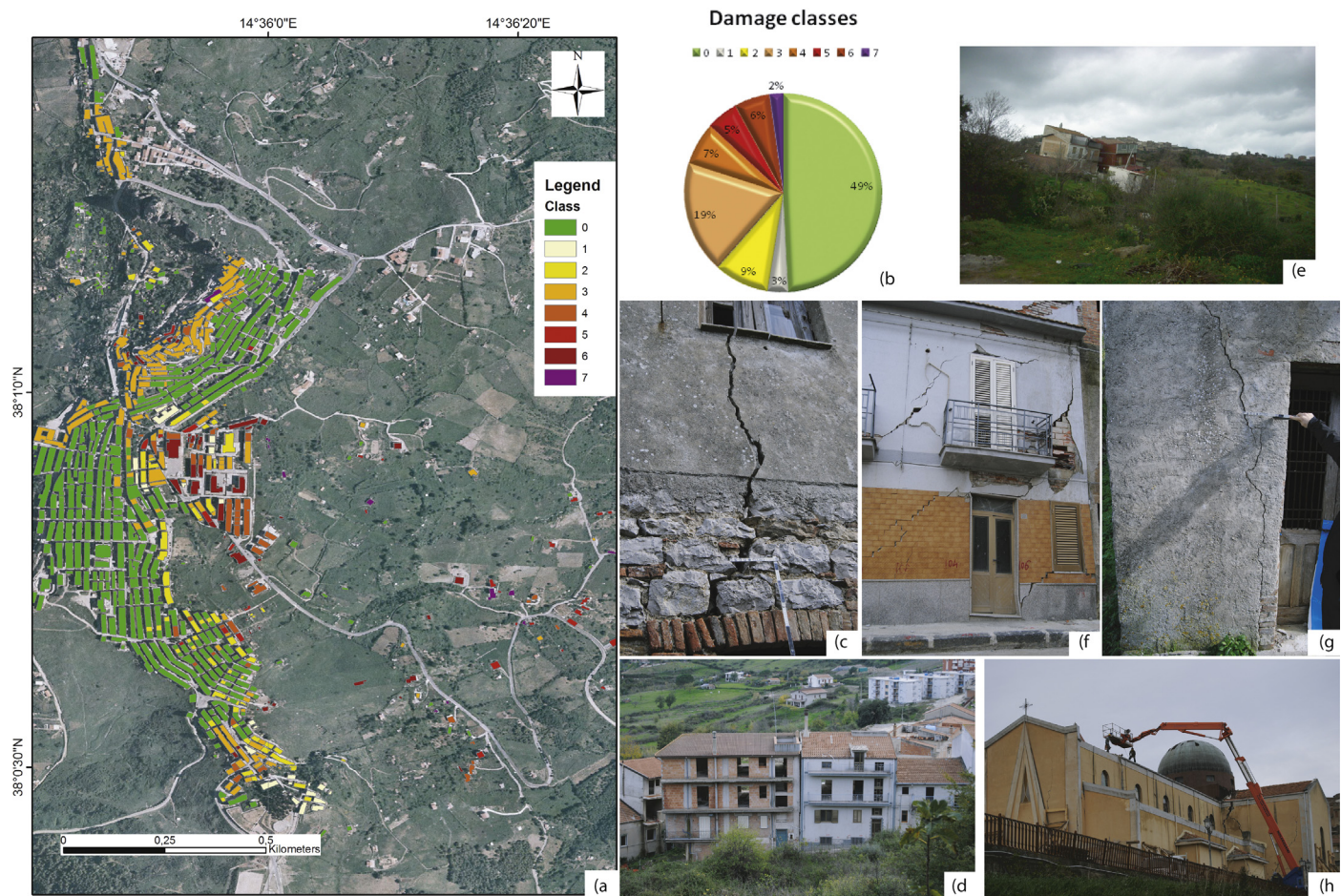


**Fig. 3.** Damage assessment map of San Fratello according to the degree of damages of Table 1 (a); and the related frequency of buildings considering the degree of damages (b). Some examples of the damages of San Fratello (c) class 3; (d) class 6; (e) class 7; (f) class 5; (g) class 2; (h) class 5.

**Table 1**  
Ranking scheme of building damage categories (modified after Cooper, 2006).

Class	
0	No damages.
1	Hairline cracking not visible from outside. Fine cracks, generally restricted to internal wall finishes: rarely visible in external brickwork. Typical crack widths up to 1 mm. Generally not visible from outside.
2	Cracks not necessarily visible externally, some external repointing may be required. Doors and windows may stick slightly. Typical crack widths up to 5 mm. Difficult to record from outside.
3	Cracks that can be patched by a builder. Repointing of external brickwork and possibly a small amount of brickwork to be replaced. Doors and windows sticking, slight tilt to walls, service pipes may fracture. Typical crack widths are 5–15 mm, or several of say 3 mm. Visible from outside.
4	Extensive damage that requires breaking-out and replacing sections of walls, especially over doors and windows. Windows and door frames distorted, floors sloping noticeably; some loss of bearing in beams, distortion of structure. Service pipes disrupted. Typical crack widths are 15–25 mm, but also depends on number of cracks. Noticeable from outside.
5	Structural damage, which requires a major repair job, involving partial or complete rebuilding. Beams lose bearing capacity, walls lean badly and require shoring. Windows broken with distortion. Danger of instability. Typical crack widths are >25 mm, but depend on the number of cracks. Very obvious from outside.
6	Partial collapse. Very obvious from outside.
7	Total collapse. Very obvious from outside.

**Table 2**  
used PS InSAR datasets.

Sensor	Geometry	Time interval	No. of scenes	Density (PS/km <sup>2</sup> )
ERS 1/2	Ascending	11/09/92–05/06/00	34	6.55
ERS 1/2	Descending	01/05/92–08/01/01	70	46.45
ENVISAT	Ascending	22/01/03–22/09/10	65	64.74
ENVISAT	Descending	07/07/03–13/09/10	49	20.41
RADARSAT	Ascending	30/012/05–26/01/10	47	85.86
RADARSAT	Descending	31/01/06–03/02/10	47	85.86
COSMOSky-Med	Descending	16/05/11–02/05/12	32	400.62
TERRASar-X	Descending	28/10/11–22/09/12	30	813



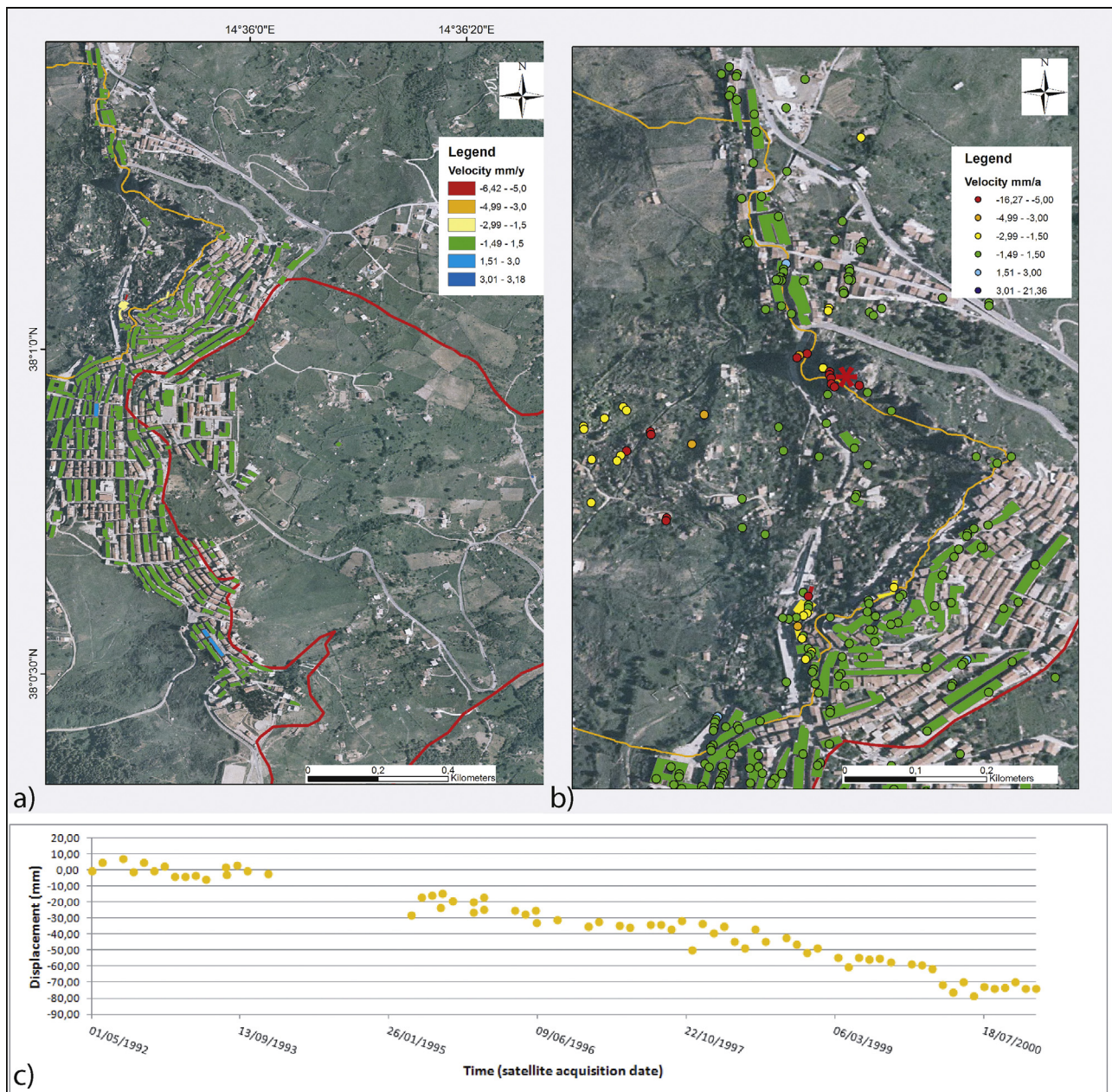


**Fig. 4.** (a) Buildings deformation velocity map obtained using ERS 1/2 descending data. (b) Details of the 1922 landslide with the PS dataset. The red asterisk stands for the PS time series of (c). The red line corresponds to the 2010 landslide boundary; the orange line corresponds to the 1922 landslide boundary.

Bianchini et al., 2014b). The oldest documented one occurred in 1754, destroying the north-eastern part of the town, medieval in age. The 8th of January 1922 another large landslide seriously damaged the north-western quarters, causing the town delocalization. The most recent landslide occurred on February 14th 2010 causing several damages to buildings and infrastructures. This landslide affected the eastern sector of the town, determining the evacuation of more than 2000 people. From a geomorphological point of view San Fratello is located at about 650 m a.s.l. along a N–S oriented divide on which both the west and east facing slopes are characterized by a steep gradient and creek erosion at their toe.

From a geological point of view, the study area is part of the collisional system, developed since the Late Cretaceous, as the result of the convergence between the European and African-Adriatic plates (Corrado et al., 2009). The study area is characterized by the presence of two main structural domains: the

Kabilian-Peloritan-Calabrian units at northeast, overthrust on the Apenninic-Maghrebian domain to the southwest (Lentini et al., 2000; Lavecchia et al., 2007). The Kabilian-Peloritan-Calabrian units are made of imbricate sheets of Paleozoic metamorphic and igneous rocks and the related Mesozoic sedimentary cover (Somma et al., 2005). These units, cropping out within the Peloritani mountains, are covered by Upper Oligocene-Lower Burdigalian deposits (Lentini et al., 2000). The Apenninic-Maghrebian domain crops out in the Nebrodi Mountains and is made of imbricate sheets of Mesozoic-Tertiary sedimentary rocks. The boundary between these two domains, corresponds to the limit between the Peloritani and Nebrodi mountain chains; this boundary is represented by an active frontal thrust marked by the Longi-Taormina lineament (Catalano et al., 2006; Billi et al., 2007). San Fratello is located in proximity to this fault (Fig. 2). The rocks outcropping within the San Fratello area consist of a Cretaceous-Oligocene terrigenous-flyschoid to



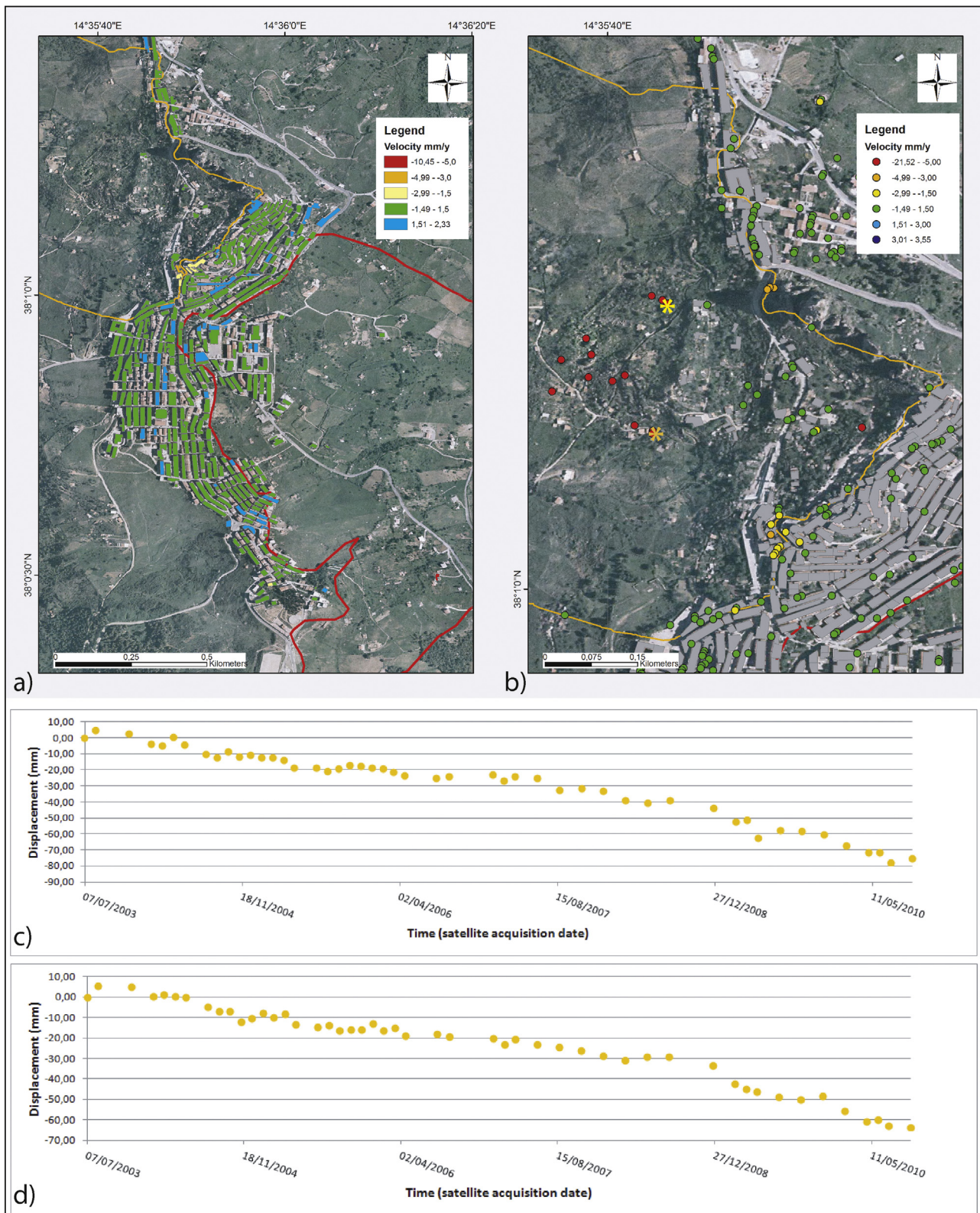


**Fig. 5.** (a) Building deformation velocity map using both ascending and descending ENVISAT datasets. (b) ENVISAT PS dataset related to the 1922 landslide with two selected time series (c and d). (c) Corresponds to the yellow asterisk; (d) corresponds to the orange asterisk.

calcareous sedimentary sequence. In particular, the western and southern part of the study area is mostly characterized by terrigenous terrains, represented by the Appenninic-Maghrebid Units (clays alternating with sandstones and clayey-marly formations).

In the northern portion of the area, the uppermost units (Kabilo-Calabride Units) crop out, occurring as Liassic carbonate platform sequences overlapped by a terrigenous Late Eocene-Oligocene Flysch. Cretaceous pelagic dolostones and limestones (San Marco



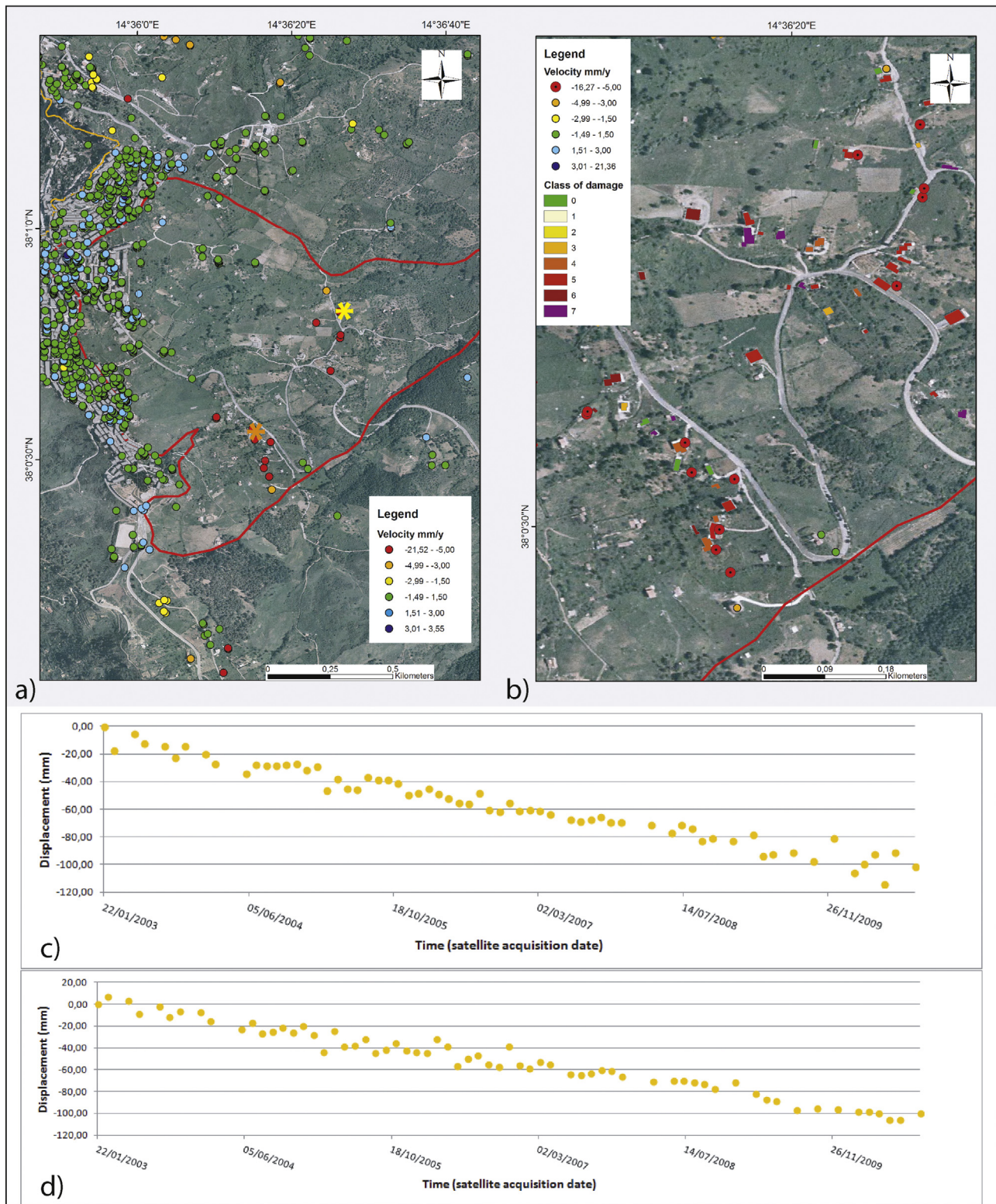


**Fig. 6.** (a) ENVISAT ascending PS dataset; (b) comparison between the ground deformation velocity map and the damage assessment map; (c) time series correspondent to the yellow asterisk; (d) time series correspondent to the orange asterisk.

D'Alunzio Unit) crop out in the N-NE sector of San Fratello (Giunta et al., 2000; Lavecchia et al., 2007). The poor geotechnical properties of the clay-silt and flyschoid lithotypes are one of the triggering factors of the landsliding phenomena, combined with the steep topography and the occurrence of intense rainfall events.

## Methodology

### Damage assessment map

The damage assessment map was performed after an accurate field survey, covering the whole town area of San Fratello. A total



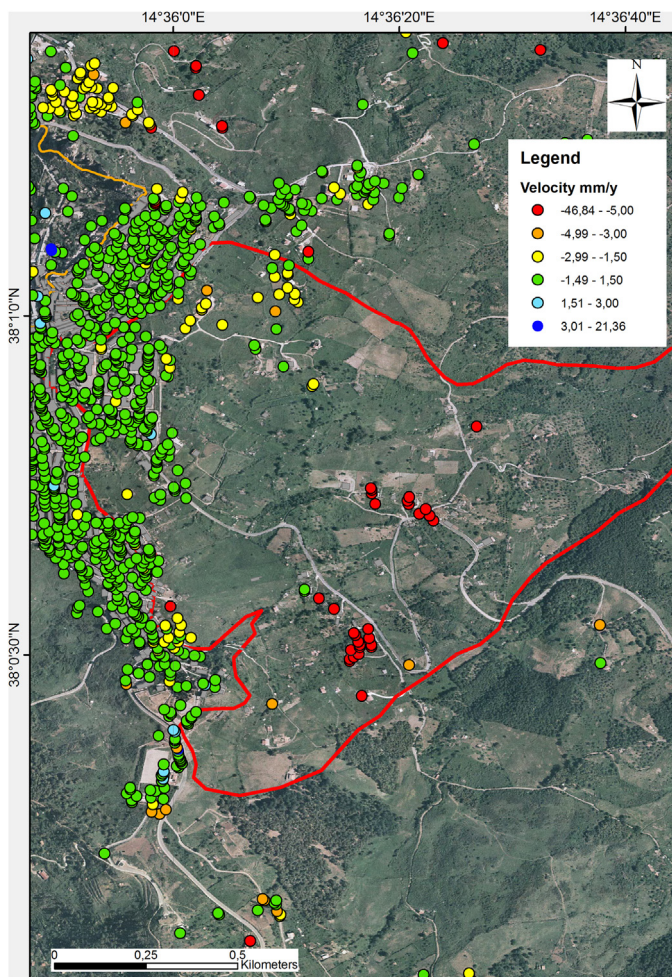


Fig. 7. Building deformation velocity map using both ascending and descending RADARSAT-1 datasets.

amount of 738 buildings were mapped on the basis of the damages observable on their walls and facades. Buildings interior damages were evaluated by interviewing the local inhabitants. The degree of damages for each building was evaluated using a modified version of ranking scheme of building damage categories of Cooper (2006) (Table 1).

#### Radar interferometry

Spaceborne Interferometric radar approach represents a powerful tool to detect movements on the Earth's surface. Mapping geomorphologic processes and monitoring slope instability can greatly benefit from satellite data analysis due to the great cost–benefits ratio, non-invasiveness, wide area coverage and high precision. Spaceborne InSAR can offer a useful support in the detection and characterization of slow surface displacements, providing rapid and easily updatable ground velocity measurements, along the satellite line of sight (LOS). Multi-interferometric InSAR technique has turned out to be a valuable and successful tool to detect and measure surface displacements with millimeter accuracy, and also to reconstruct the deformation history of the investigated areas (Bovenga et al., 2006; Colesanti and Wasowski, 2006; Cascini et al., 2009; Cigna et al., 2011; Hung et al., 2011; Bianchini et al., 2012; Ciampalini et al., 2012; Raspini et al., 2012; Del Ventisette et al., 2014; Bianchini et al., 2014b). In the last 20 years, several different radar satellite missions were launched, providing different

types of SAR images to be used for ground movement detection and monitoring. Consequently, today many satellite interferometric data are available, including both historical archives, acquired since the early 1990s (e.g. ERS 1/2, ENVISAT), and images from currently operating satellites (e.g. TerraSAR-X, COSMO-SkyMed), spanning a time interval of more than 20 years, which can allow the analysis of both past and recent ground displacements of the observed scenes (Bianchini et al., 2012). PSInSAR can be used to analyze archival SAR data, providing annual velocities and deformation time series on grids of stable reflective point-wise targets, called Persistent Scatterers (PS), characterized by a coherent electromagnetic behavior in all the radar images (Ferretti et al., 2001). Several of these PS correspond to hand-made artifacts, such as buildings, railways or highways, making this method suitable for the monitoring of urbanized areas where the density of the PS is higher. This can provide exclusive information for an improved understanding of the long term behavior of slow and very-slow ground deformation phenomena (Del Ventisette et al., 2013). PSI analysis, properly integrated with auxiliary data, has been mainly used for mapping and monitoring slow-moving landslides, and for evaluating their state of activity and intensity (Ferretti et al., 2000; Meisina et al., 2008; Herrera et al., 2009, 2010; Guzzetti et al., 2009; Notti et al., 2010; Righini et al., 2012; Bianchini et al., 2014b). The recorded displacements are measured considering a ground point of known coordinates, called reference point, considered stable on the basis of the geological knowledge of the area. Satellite sensors are side-looking and acquire images in two different geometries, following an approximately N–S direction and a perpendicular line of sight (LOS). For this reason, sensors moving from south to north acquire in ascending geometry and are more suitable to detect movements located on west facing slopes. On the contrary, sensors moving from north to south acquire in descending geometry making them suitable for the observation of east-facing slopes. Five different sensors were used to monitor the buildings of San Fratello: ERS 1/2, ENVISAT, RADARSAT-1, COSMO-SkyMed (CSK) and TerraSAR-X (TSX) (Table 2) covering a very long interval of time, spanning from 1992 up to 2012. Satellite SAR data were processed by T.R.E. (Tele Rilevamento Europa). The ground deformation velocity of each building was calculated considering the average velocity of all the PS included in the polygon corresponding to the building. The calculation was performed for each C- and X-band dataset. To avoid problems related to a possible shift between the buildings and the PSI layers, due to a non-extremely accurate georeferencing process, PS located in a range of 2 m outside the buildings were included in the calculation of the average velocity. Furthermore, the use of these 2 m wide buffer improved the number of usable PS. Considering the ground deformation velocity, a stability threshold was chosen between  $\pm 1.5$  mm/y for the C-band data and  $\pm 2$  mm/y for the X-band data. These thresholds were decided on the basis of both the investigated phenomena (slow moving) and the standard deviation of the PS population.

## Results

#### Damage assessment map

The damage assessment map (Fig. 3) reports the degree of damages of a total of 738 buildings classified following the scheme reported in Table 1. The map shows that more than half of San Fratello buildings are affected by damages caused by slope instability; amongst them 20% of buildings are strongly damaged (more than class 4). The most affected areas are located on the town eastern slope, within the Stazzone quarter and East of the city center (Fig. 3a). In these areas, also some of the most recent buildings collapsed or were damaged to the point that they required to be



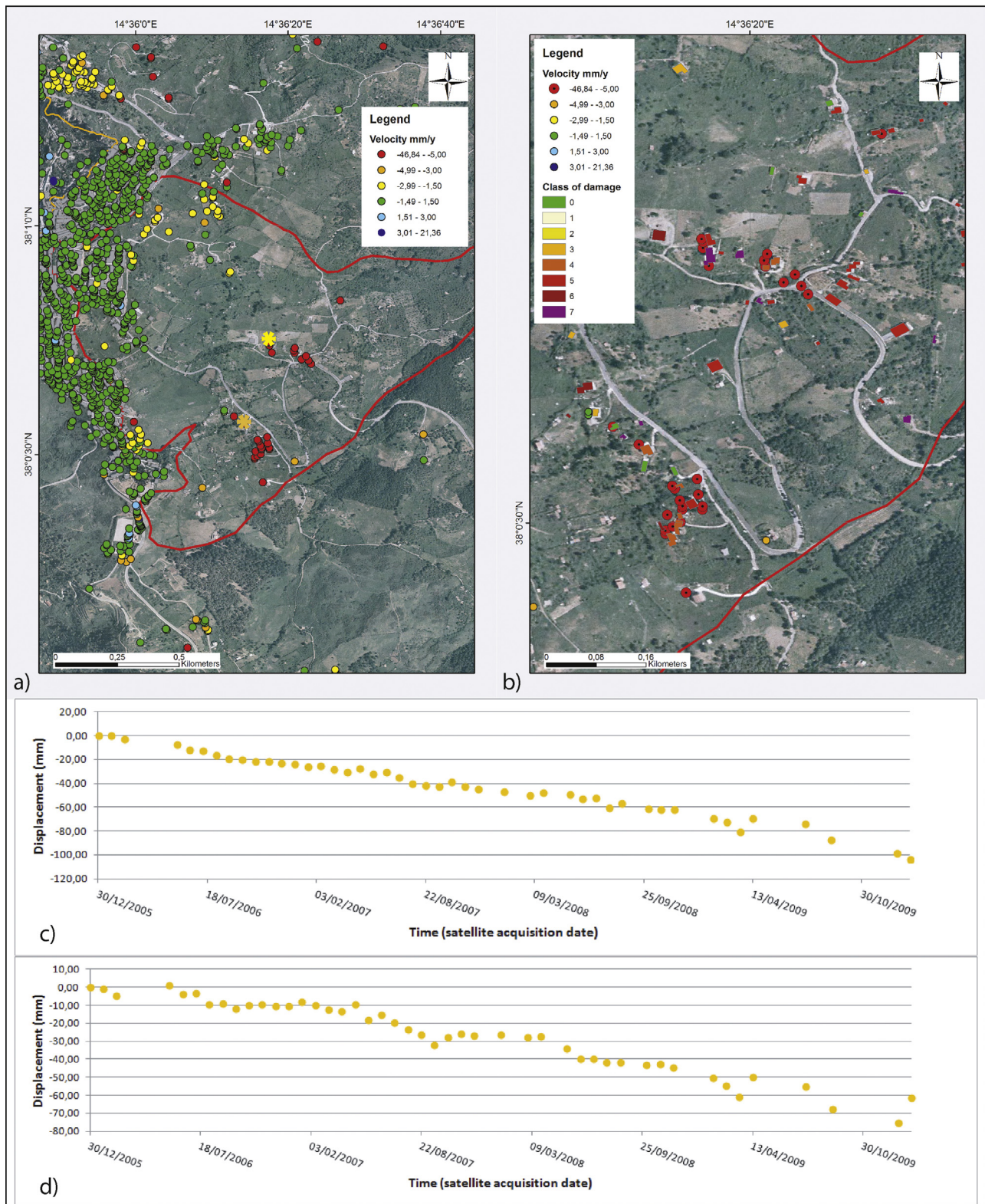


**Fig. 8.** (a) RADARSAT-1 ascending PS dataset; (b) comparison between the ground deformation velocity map and the damage assessment map; (c) time series correspondent to the yellow asterisk; (d) time series correspondent to the orange asterisk.

demolished. Intense damages can be observed also in the Riana and San Benedetto quarters along the 2010 landslide crown (Fig. 3e). The field surveys revealed also the presence of several damaged buildings located in the northwestern part of town, corresponding to the 1922 landslide crown area.

#### Radar interferometry

##### ERS 1/2 (1992–2001)

The buildings deformation velocity maps using the ERS 1/2 datasets highlight that no buildings located in the area of the 2010



landslide are affected by deformation, however a maximum of 178 (24.12%) buildings were mapped using the descending dataset (Fig. 4a). Along the 1922 landslide crown, some buildings show a deformation velocity, which is consistent with the damages observed on their walls and facades. In this case, the extent of the area affected by deformation is underestimated. A better result can be obtained by the observation of the whole PS dataset (Fig. 4b). PS targets clearly show the presence of at least two other areas characterized by ground deformation, one located along the 1922 landslide crown (Fig. 4a), where the mean deformation velocity is up to  $-9$  mm/y (Fig. 4b and c), and another one within the landslide body (Fig. 4b).

#### ENVISAT (2003–2010)

The use of the ENVISAT datasets allowed the mapping of up to 279 (37.80%) of the town buildings. The related building deformation velocity map (Fig. 5a) is very similar to those obtained with ERS 1/2 datasets. Results highlight a substantial stability of the town. A very small amount of buildings is characterized by deformation velocities outside the stability range. Along the eastern slope, only one edifice shows an average velocity of  $-10$  mm/y. On the western slope, along the 1922 landslide crown, the buildings affected by deformation are almost the same of those highlighted by the map obtained with ERS 1/2. The use of ENVISAT sensor increased the number of monitored buildings; however, these PS data were still not suitable to detect possible ground displacements to be considered as landslide precursors. Also in this case using the whole PS datasets it was possible to retrieve more information about slope instability (Fig. 5b). Along the western town sector the area affected by ground deformation could be better recognized using PS which highlighted the presence of a wide area affected by deformation, located along in the eastern sector of the 1922 landslide (Fig. 5b). The most interesting information obtained using the ENVISAT data concerns the ground deformation of the eastern slope (Fig. 6a). Here two areas, showing clusters of PS characterized by high ground deformation velocities, can be recognized. Even though both these areas are located inside the 2010 landslide body, including a very low number of buildings, the number of PS is sufficient to highlight ground deformation. The comparison between the PS and the damage assessment map shows a good agreement between the distribution of the PS having the highest velocities and the most damaged buildings by the 2010 landslide (Fig. 6b).

#### RADARSAT-1 (2005–2010)

RADARSAT-1 data can be used to confirm the results obtained by ENVISAT data due to the partial overlapping of their temporal coverage. The main advantage of the use of RADARSAT-1 is represented by the higher density of PS that allows mapping the deformation velocity of almost the half (48.37%) of the monitored buildings. Results clearly highlight three areas where buildings are affected by deformation (Fig. 7). The first area is located within the eastern slope, confirming the results of ENVISAT data. In addition, the deformation of the edifices located along the 1922 landslide crown is confirmed. The third area corresponds to the San Benedetto quarter, where four buildings show velocities slightly higher than the stability range. Considering the whole PS RADARSAT-1 ascending dataset (Fig. 8a), the area affected by ground deformation located within the eastern slope is clearly recognizable. Also, in this case, the agreement between the ground deformation velocities and the damage assessment map is good (Fig. 8b), confirming the usefulness of the C-band sensors relatively to this area, where the buildings affected by severe damages are surrounded by PS showing the highest velocities. Also along the western slope, RADARSAT-1 confirms the results obtained by ENVISAT highlighting the presence of ground deformation within the body and along the 1922 landslide crown.

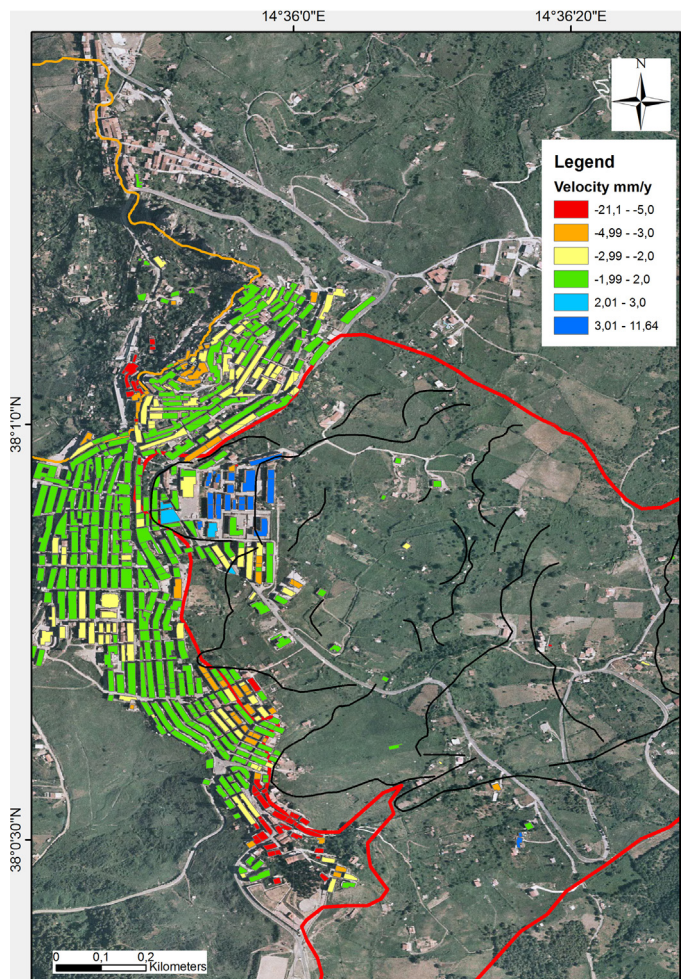
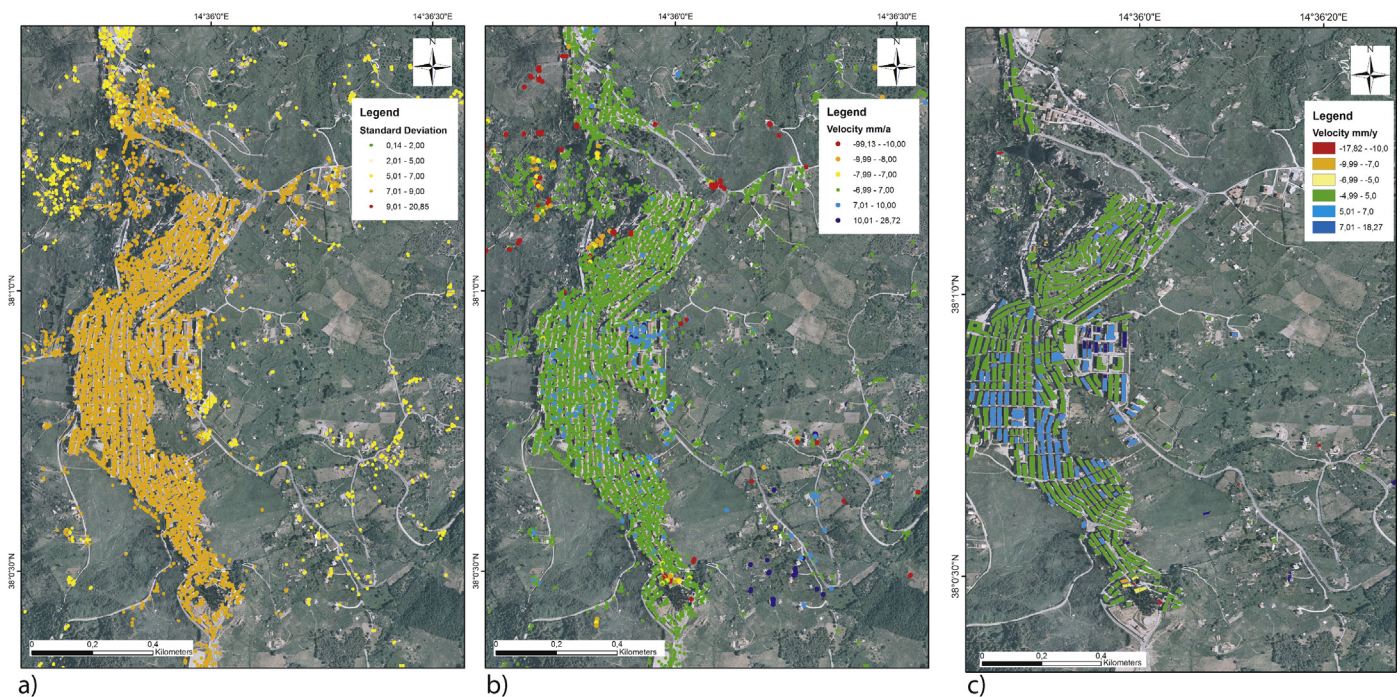


Fig. 9. Building deformation velocity map using both ascending and descending COSMO-SkyMed datasets. The black lines correspond to the secondary scarps developed during the 2010 landslide.

#### COSMO-SkyMed (2011–2012)

CSK images were acquired after the 2010 landslide, thus they can be useful to evaluate possible post-event ground deformation phenomena. The available data were acquired only in descending orbit, making them suitable especially to study the deformation of the western slope. Anyway, the high density of the PS allowed to retrieve also interesting information about the eastern slope deformation. The stability range for CSK data was increased to  $\pm 2$  mm/y because of the higher average standard deviation of PS velocity, if compared to those of the C-band data. The increase of the standard deviation is related to the short acquisition period (only one year) and to the location of San Fratello, which turns out to be far from the reference point and at the boundary of the used SAR images. In this case, the building deformation velocity map permits to recognize three different areas (Fig. 9), along the 2010 landslide crown, where several buildings are affected by a considerable deformation. These areas correspond, from north to south, to the Stazzone, Riana and San Benedetto quarters, which were intensely damaged during the event. The difference in colors between the Stazzone and San Benedetto quarters, that represent different displacement direction, is related to the different position of the areas within the 2010 landslide. Buildings that are moving toward the satellite characterize Stazzone quarter, whereas in San Benedetto the edifices are moving away with respect to the sensor. The first ones are located inside the landslide body, whereas the second ones are placed along the landslide crown.





**Fig. 10.** Standard deviation (a), ground deformation velocity map with  $\pm 7$  mm/y stability range (b) and building deformation velocity map with  $\pm 5$  mm/y stability range (c) using the descending TerraSAR-X dataset.

The fractures patterns developed on the building facades suggest that Stazzzone is moving downhill, on the contrary part of the building located within the San Benedetto is characterized by mainly vertical movement. This is consistent with the geometry of the landslide, which is rotational in the upper part and translational downward. Another interesting result is represented by the presence of a strip, located along the crown of the 1922 landslide, characterized by several buildings showing high deformation velocities. These edifices present well developed fractures on their facades, confirming that this area is interested by slow but continuous ground deformation. The comparison between the building deformation velocity map, obtained using CSK data, and the damage assessment map shows a very good agreement, confirming that the most intensely damaged area during the 2010 landslide are, today, characterized by residual movements, which compromise their stability. Several of these buildings were recently evacuated and some of them completely demolished. The measurement of the velocities related to residual movements must be used with caution because of the high standard deviation.

#### *TerraSAR-X (2011–2012)*

The available TSX data were acquired between October 2011 and December 2012. Part of the acquisition period is overlapped with that of the CSK data. This dataset is affected by a very high standard deviation, especially in correspondence of San Fratello town area, where the average standard deviation is 7.6 (Fig. 10a and b). These high values depend on several factors (e.g. the choice of the reference point, the short acquisition period, the topographic factor and the position of the area, located close to the boundary of the SAR images). For these reasons, TSX data could not be used to calculate the building deformation velocities. However, some consideration about the ground deformation can be made considering as not moving the areas resulting stable from CSK. A differential analysis can be useful to highlight areas affected by ground deformation. In this case, the applied stability threshold was selected between  $\pm 7$  mm/y, considering the standard deviation. Results suggest that almost three areas of the town are affected by ground deformation:

the northern one is located along the crown of the 1922 landslide, the second one is represented by part of the Stazzzone quarter and the southern one corresponds to the San Benedetto quarter (Fig. 10c). Ground displacements highlighted by TSX confirm the results obtained using CSK but, considering the standard deviation, the evaluation of the ground deformation velocities can be made only with the last one.

#### *Reprocessed X-band data*

Considering the interesting results highlighted by X-band sensors, the TSX and CSK datasets were reprocessed, choosing a different reference point, in order to minimize the standard deviations. The new reference points were located inside San Fratello, in correspondence of buildings considered stable. This procedure allowed a more accurate measurement of building deformations velocities. During the reprocessing of the CSK data, several PS, located in the western part of the town were lost, but the building deformation velocity map clearly shows that Stazzzone and San Benedetto quarters are affected by important deformations (Fig. 11). In addition the reprocessed TSX data (Fig. 12) confirmed that these two areas are subjected to ground deformations, especially San Benedetto where the extent, the geometry of the deformations and the average velocities are comparable to the CSK data. TSX data can be useful also to observe the deformations located along the western slope, where several buildings show high velocities.

#### **Discussion**

Landslides may affect different kind of buildings in different ways. Construction methods, with regard to depth of foundations and used material, can counteract the development of the damages caused by ground displacement. This fact is fundamental to be taken into account in a town such as San Fratello, where very different kinds of buildings are present. San Fratello town is composed by historical buildings made of bricks, having very shallow foundations, as well as recent buildings with deeper foundations and



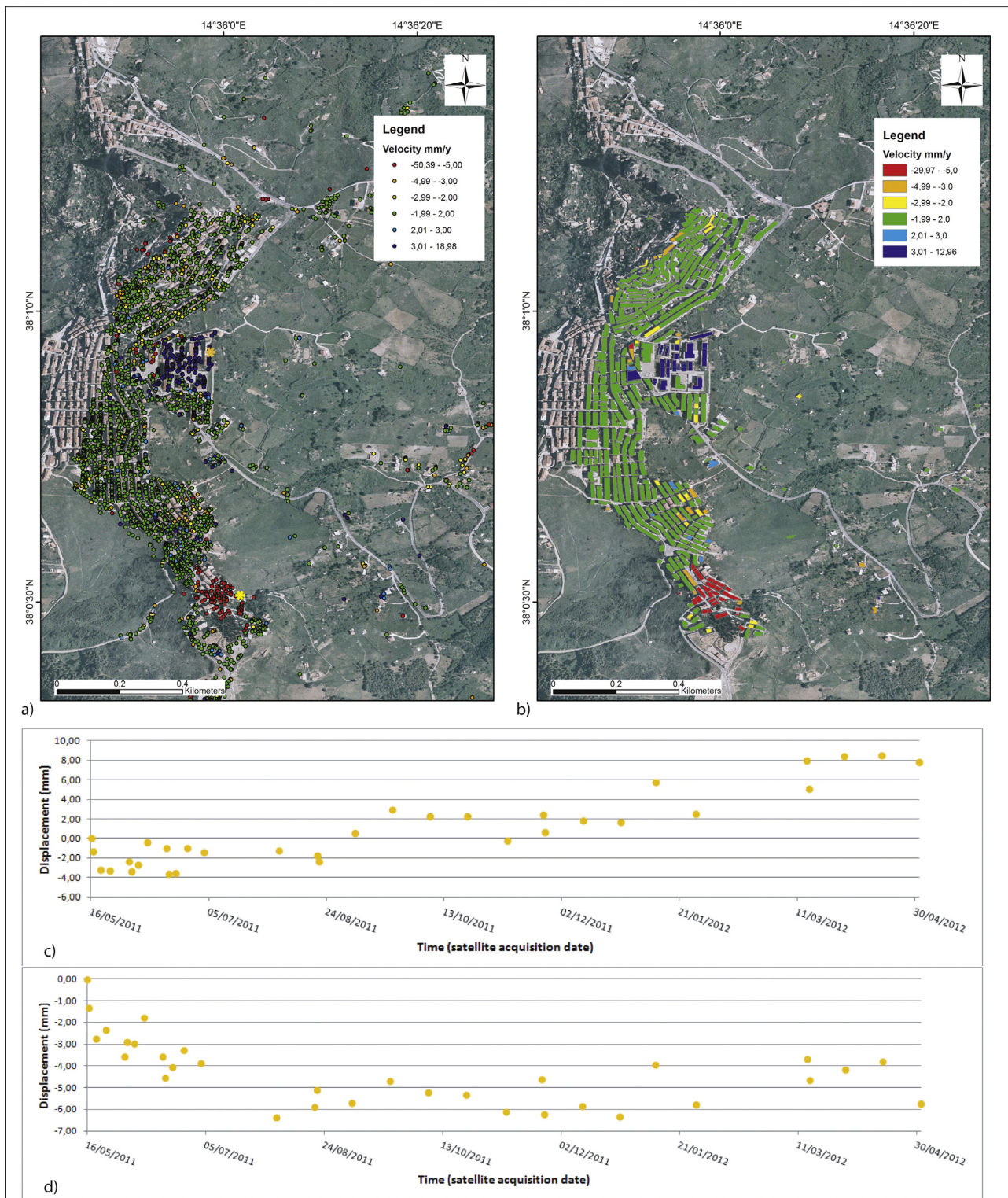


**Fig. 11.** (a) CSK ground deformation velocity map; (b) building deformation velocity map obtained by using CSK data; (c) time series correspondent to the orange asterisk and (d) time series correspondent to the yellow asterisk.

a reinforced concrete structure. After the 2010 landslide the first ones show various degrees of damages, going from well-developed fractures on their walls and facades, distortion of windows and door frames, up to the structural partial or total collapse (Fig. 3). The more recent buildings stood up well to the landslide induced deformations, but in some cases, they show a rotation of the whole structure. The combined use of the buildings map and the PS radar

datasets (Table 3) highlighted that the PS density is a fundamental parameter in order to evaluate the feasibility of this application for building monitoring activities. Only the X-band datasets, bearing a high target density ( $\gg 200$  PS/km<sup>2</sup>), resulted useful to understand the displacement velocities of at least more than the half of the buildings of the San Fratello town. Anyway, some information were also retrieved by RADARSAT-1 datasets. The number of



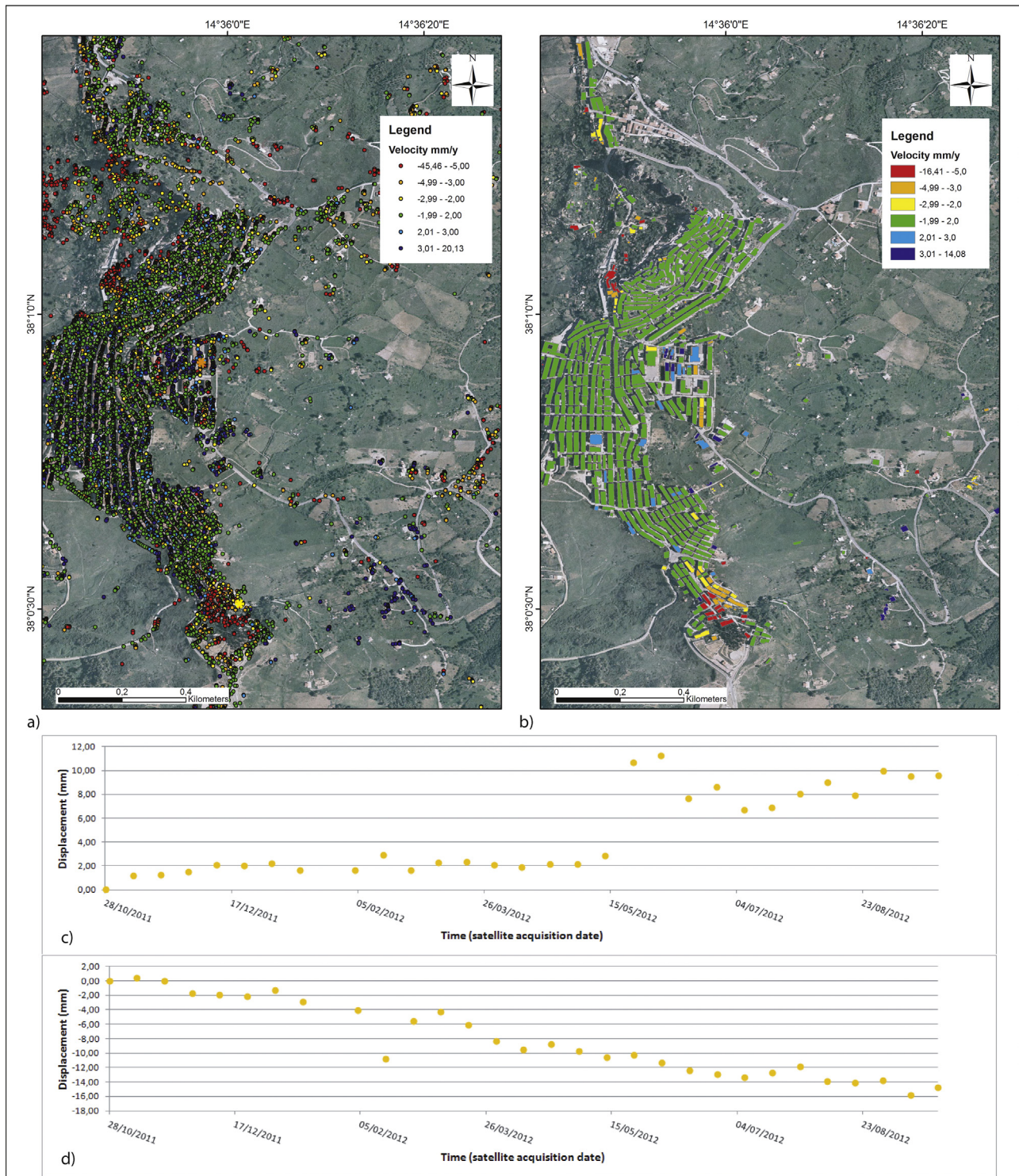


**Fig. 12.** (a) TSX ground deformation velocity map; (b) building deformation velocity map obtained by using TSX data; (c) time series correspondent to the orange asterisk and (d) time series correspondent to the yellow asterisk.

monitored buildings was sensibly improved considering a buffer of 2 m for each building. The size of the buffer was decided considering the proximity among the buildings. A wider buffer can lead to consider PS belonging to another building, especially in the city center, where several streets are very narrow. The use of a 2 m wide buffer allowed a considerable PS number improvement, which were used to calculate the buildings deformation velocity (Table 4). This improvement was observed for all the dataset even if

the C-band sensors (ERS 1/2 and ENVISAT) were still characterized by a low percentage of monitored buildings. Only RADARSAT-1, among the C-band sensors, permitted the monitoring of a sufficient amount of buildings. When the percentages of monitored buildings were less than 40%, the use of the whole PS dataset was considered more appropriate in order to avoid the loss of information. The comparison between the building deformation velocity maps, highlights that before the 2010 event, all the C-band satellites



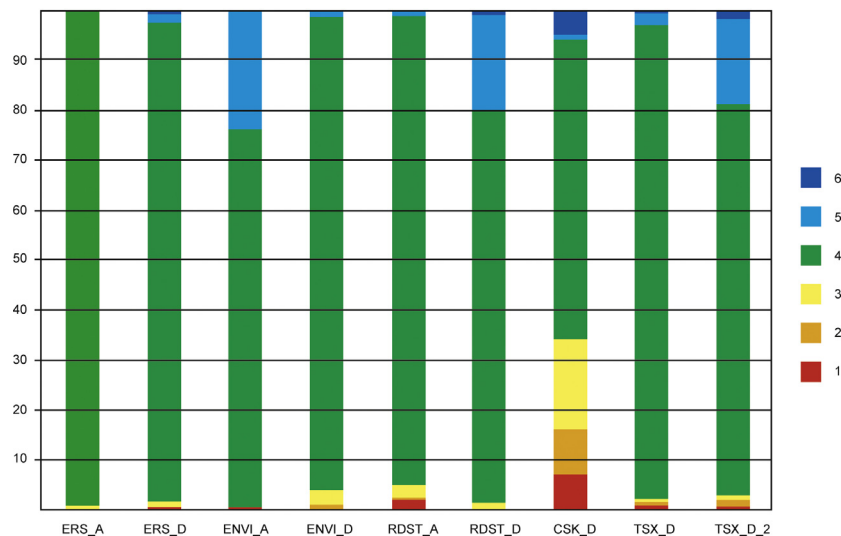


**Fig. 13.** Percentages of buildings monitored with the available sensors considering the used velocity (in mm/y) classification described in the previous paragraphs. For C-band sensors: class 1:  $<-5$ ; class 2:  $-4.99$  to  $-3.00$ ; class 3:  $-2.99$  to  $-1.5$ ; class 4:  $-1.49$  to  $1.5$ ; class 5:  $1.51$ – $3.00$ ; class 6:  $>3$ . For CSK: class 1:  $<-5$ ; class 2:  $-4.99$  to  $-3.00$ ; class 3:  $-2.99$  to  $-2.0$ ; class 4:  $-1.99$  to  $2.0$ ; class 5:  $2.01$ – $3.00$ ; class 6:  $>3$ . For TSX.D: class 1:  $<-10$ ; class 2:  $-9.99$  to  $-8.00$ ; class 3:  $-7.99$  to  $-7.0$ ; class 4:  $-6.99$  to  $7.0$ ; class 5:  $7.01$ – $9.00$ ; class 6:  $>9$ ; for TSX.D.2: class 1:  $<-10$ ; class 2:  $-9.99$  to  $-7.00$ ; class 3:  $-6.99$  to  $-5.0$ ; class 4:  $-4.99$ – $5.0$ ; class 5:  $5.01$ – $7.00$ ; class 6:  $>7$ .

**Table 3**

Results of the interpolation between the considered PS datasets and the buildings map using a simple intersection.

Dataset	No. of PS	PS/km <sup>2</sup>	No. of buildings	%
ERS 1/2.asc	63	35	45	6.10
ERS 1/2.desc	247	137.2	128	17.34
ENVISAT.asc	418	232.2	199	26.97
ENVISAT.desc	115	63.89	75	10.16
RADARSAT-1.asc	298	165.56	203	27.51
RADARSAT-1.desc	480	266.67	259	35.10
COSMO-SkyMed.desc	1447	803.89	405	54.95
TerraSAR-X	1567	870.56	442	59.98

**Table 4**

Results of the interpolation between the considered PS datasets and the buildings map using an intersection with a 2 m tolerance.

Dataset	No. of PS	PS/km <sup>2</sup>	No. of buildings	%
ERS 1/2.asc	149	82.22	101	13.69
ERS 1/2.desc	359	199.44	178	24.12
ENVISAT.asc	634	352.22	279	37.80
ENVISAT.desc	310	172.22	170	23.04
RADARSAT-1.asc	653	362.78	357	48.37
RADARSAT-1.desc	757	420.56	348	47.15
COSMO-SkyMed.desc	3036	1686.67	506	68.56
TerraSAR-X	4718	2621.11	608	82.38

indicate a substantial stability of the town (Fig. 13). In particular, up to the 96% of the monitored buildings with ERS 1/2 are characterized by velocities included within the stability range. Despite of the low number of monitored edifices, the ground deformation velocity maps for the eastern slope also confirm these results: no significant deformations were observed. The number of buildings affected by higher deformation velocities increases considering ENVISAT and RADARSAT-1. This increase can be related to the higher PS density. The ground deformation velocity maps obtained using ENVISAT and RADARSAT-1 suggest that the area corresponding to the 2010 landslide body was affected by ground deformation. Thanks to the higher PS density of RADARSAT-1, the instability can be also appreciated in the related building deformation velocity map. The number of buildings affected by deformation increases sensibly considering the X-band sensors, especially with regards to CSK, which highlights that only 60% of the monitored buildings are

characterized by velocities within the stability range. These results are confirmed by the comparison between the building deformation velocity map and the damage assessment map. Buildings characterized by the highest residual velocities are located in the area affected by the 2010 landslide. A direct correlation between the deformation velocity and the degree of the damage was not observed because of the type of building affects their response to the deformation. For example, modern buildings having reinforced concrete foundations better resist to the stress with respect to the historical buildings. The X-band data highlighted the presence of considerably residual movements along the eastern slope even two years after the event. TSX data can be used with caution because of their high standard deviation, which makes PS velocities not reliable. Only a differential analysis can be performed to highlight moving areas with respect to stable areas. The TSX building deformation velocity map confirmed the same areas affected by ground deformation detected by CSK. An improvement in the measured velocities accuracy was obtained thanks to the reprocessing of the X-band datasets. Using these datasets, it was possible to reduce the standard deviation and to evaluate the deformation velocities more accurately. Interesting results were obtained also along the 1922 landslide crown. In this area, slow but continuous deformation was detected since 1992. In this sector, the correlation between the damaged buildings and the building deformation velocity map is very high. Some evidences of deformations of the edifices can be observed also using C-band sensors, but the lower PS density suggests that the use of the ground deformation velocity map is more suitable.

## Conclusions

PSInSAR technique, using five different sensors, was successfully used to evaluate the building deformation velocities of the San Fratello municipality, which was affected by two landslides occurred in 1922 and 2010 respectively. The C-band data were acquired before the 2010 event, in order to observe the presence of landslide precursory symptoms, whereas X-band satellite radar data were acquired during the post event phase, with the aim of detecting the landslide residual risk.

The advantages of the X-band data are represented by the high PS density, which allowed to measure the deformation velocity of



a large number of the surveyed buildings (more than 80%). On the contrary, the C-band satellites were characterized by a low percentage of mapped edifices. Only RADARSAT-1 data seemed to be effective in order to understand possible presence of deformation areas within the San Fratello town. The low density of the C-band sensors suggests that the use of the ground deformation velocity map is more suitable with respect to the building deformation velocity map. Using the latter, several information about ground deformation can be lost, in case of several PS do not correspond to buildings. Usually X-band SAR images are most expensive but, at the local scale, the advantages of the higher PS density is much greater in terms of obtained results.

This work proves the effectiveness of the combined use of ground and building deformation velocity maps to understand the behavior of landslide phenomena during the pre- and post-event management phase. In particular X-band data, applied to the monitoring of building deformation, combined with the damage assessment map, can be profitably used by the Civil Protection and local Authorities during the post event, in order to evaluate the residual risk and to plan evacuation procedures and mitigation measures regarding the most damaged and unstable buildings. This work also highlights the importance of the continuous monitoring of urbanized areas affected by slope instability phenomena. In this case, the long term monitoring was performed using five different sensors, but this approach can be relevant to the design of future products based on data routinely acquired by the new ESA Sentinel mission.

## Acknowledgements

The research leading to these results received funding from the European Union Seventh Framework Program (FP7/2007–2013) under grant agreement No. 242212 (Project DORIS) and Project LAMPRE. We also thank two anonymous reviewers for the helpful suggestions.

## References

- Bianchini, S., Cigna, F., Righini, G., Proietti, C., Casagli, N., 2012. *Landslide hotspot mapping by means of persistent scatterer interferometry*. *Environ. Earth Sci.* 67 (4), 1155–1172.
- Bianchini, S., Tapete, D., Ciampalini, A., Di Traglia, F., Del Ventisette, C., Moretti, S., Casagli, N., 2014a. *Multi-temporal evaluation of landslide-induced movements and damage assessment in San Fratello (Italy) by means of C- and X-band PSI data*. In: Pardo-Igúzquiza, E., Guardiola-Albert, C., Heredia, J., Moreno-Merino, L., Durán, J.J., Vargas-Guzmán, J.A. (Eds.), *Mathematics of Planet Earth*. Springer, Berlin/Heidelberg, pp. 257–261.
- Bianchini, S., Ciampalini, A., Raspini, F., Bardi, F., Di Traglia, F., Moretti, S., Casagli, N., 2014b. *Multi-temporal evaluation of landslide movements and impacts on buildings in San Fratello (Italy) by means of C-band and X-band PSI data*. *Pure Appl. Geophys.* <http://dx.doi.org/10.1007/s00024-014-0839-2>.
- Billi, A., Presti, D., Faccenna, C., Neri, G., Orecchio, B., 2007. *Seismotectonics of the Nubia plate compressive margin in the South Tyrrhenian Region, Italy: clues for subduction inception*. *J. Geophys. Res.* 112 (B08302), <http://dx.doi.org/10.1029/2006JB004837>.
- Bovenga, F., Nutricato, R., Refice, A., Wasowski, J., 2006. *Application of multi-temporal differential interferometry to slope instability detection in urban/peri-urban areas*. *Eng. Geol.* 88, 219–240.
- Cascini, L., Fornaro, G., Peduto, D., 2009. *Analysis at medium scale of low-resolution DInSAR data in slow-moving landslide-affected areas*. *ISPRS J. Photogram. Rem. Sens.* 64 (6), 598–611.
- Catalano, S., De Guidi, G., Lanzafame, G., Monaco, C., Torrisi, S., Tortorici, G., Tortorici, L., 2006. *Inversione tettonica positiva Tardo-Quaternaria nel Plateau Ibleo (Sicilia SE)*. *Rendiconti Della Soc. Geol. Ital.* 2, 118–120.
- Cigna, F., Del Ventisette, C., Liguori, V., Casagli, N., 2011. *Radar-interpretation of InSAR time series and 'back monitoring' of ground deformation for mapping, characterization and mitigation of geological risk in urban area*. *Nat. Haz. Earth Syst. Sci.* 11, 865–881.
- Ciampalini, A., Cigna, F., Del Ventisette, C., Moretti, S., Liguori, V., Casagli, N., 2012. *Integrated geomorphological mapping in the north-western sector of Agrigento (Italy)*. *J. Maps* 8 (2), 136–145.
- Colesanti, C., Wasowski, J., 2006. *Investigating landslides with space-borne Synthetic Aperture Radar (SAR) Interferometry*. *Eng. Geol.* 88, 173–199.
- Cooper, A.H., 2006. *The classification, recording, databasing, and use of information about building damage caused by subsidence and landslides*. *Q. J. Eng. Geol. Hydrogeol.* 41, 409–424.
- Corrado, S., Aldega, L., Balestrieri, M.L., Maniscalco, R., Grasso, M., 2009. *Structural evolution of the sedimentary accretionary wedge of the alpine system in Eastern Sicily: Thermal and thermochronological constraints*. *Geol. Soc. Am. Bull.* 11–12, 1475–1490.
- Costantini, M., Iodice, A., Magnapane, L., Pietranera, L., 2000. *Monitoring terrain movements by means of sparse SAR differential interferometric measurements*. In: *Proc. IGAARSS, Honolulu, USA*, pp. 3225–3227.
- Crosetto, M., Monserrat, O., Cuevas, M., Crippa, B., 2011. *Spaceborne Differential SAR interferometry: data analysis tools for deformation measurement*. *Rem. Sens.* 3, 305–318.
- Del Ventisette, C., Garfagnoli, F., Ciampalini, A., Battistini, A., Gigli, G., Moretti, S., Casagli, N., 2012. *An integrated approach to the study of catastrophic debris-flows: geological hazard and human influence*. *Nat. Haz. Earth Syst. Sci.* 12 (9), 2907–2922.
- Del Ventisette, C., Ciampalini, A., Manunta, M., Calò, F., Paglia, L., Ardizzone, F., Mondini, A.C., Reichenbach, P., Mateos, R.M., Bianchini, S., Garcia, I., Fusi, B., Villó Deak, Z., Radi, K., Graniczny, M., Kowalski, Z., Piatkowska, A., Przylucka, M., Retzo, H., Strozzi, T., Colombo, D., Mora, O., Sanchez, F., Herrera, G., Moretti, S., Casagli, N., Guzzetti, F., 2013. *Exploitation of large archives of ERS and ENVISAT C-band SAR data to characterize ground deformation*. *Rem. Sens.* 5, 3896–3917.
- Ferretti, A., Prati, C., Rocca, F., 2000. *Nonlinear subsidence rate estimation using permanent scatterers in differential SAR interferometry*. *IEEE Trans. Geosci. Rem. Sens.* 38, 2202–2212.
- Ferretti, A., Prati, C., Rocca, F., 2001. *Permanent scatterers InSAR interferometry*. *IEEE Trans. Geosci. Rem. Sens.* 39 (1), 8–20.
- Del Ventisette, C., Righini, G., Moretti, S., 2014. *Multitemporal landslide inventory map updating using spaceborne SAR analysis*. *Int. J. Appl. Earth Obs. Geoinf.* 30, 238–246.
- Giunta, G., Nigro, F., Renda, P., Giorgianni, A., 2000. *The Sicilian-Maghrebides Tyrrhenian Margin: a neotectonic evolutionary model*. *Ital. J. Geosci.* 119, 553–565.
- Goswami, R., Mitchell, N.C., Brocklehurst, S.H., 2011. *Distribution and causes of landslides in the eastern Peloritani of NE Sicily and western Aspromonte of SW Calabria, Italy*. *Geomorphology* 132, 111–122.
- Guzzetti, F., Carrara, A., Cardinali, M., Reichenbach, P., 1999. *Landslide hazard evaluation: a review of current techniques and their application in a multi-scale study, Central Italy*. *Geomorphology* 31, 181–216.
- Guzzetti, F., Manunta, M., Ardizzone, F., Pepe, A., Cardinali, M., Zeni, G., Reichenbach, P., Lanari, R., 2009. *Analysis of ground deformation detected using the SBAS-DInSAR technique in Umbria*. *Pure Appl. Geophys.* 166 (8–9), 1425–1459.
- Guzzetti, F., Mondini, A.C., Cardinali, M., Fiorucci, F., Santangelo, M., Chang, K.T., 2012. *Landslide inventory maps: new tools for an old problem*. *Earth-Sci. Rev.* 112 (1–2), 42–66.
- Herrera, G., Davalillo, J.C., Cooksley, G., Monserrat, O., Pancioli, V., 2009. *Mapping and monitoring geomorphological processes in mountainous areas using PSI data: Central Pyrenees case study*. *Nat. Haz. Earth Syst. Sci.* 9, 1587–1598.
- Herrera, G., Tomás, R., Monells, D., Centolanza, G., Mallorqui, J.J., Vicente, F., Navarro, V.D., Lopez-Sanchez, J.M., Sanabria, M., Cano, M., Mulas, J., 2010. *Analysis of subsidence using TerraSAR-X data: Murcia case study*. *Eng. Geol.* 116, 284–295.
- Herrera, G., Gutierrez, F., Garcia-Davalillo, J.C., Guerrero, J., Notti, D., Galve, J.P., Fernandez-Merodo, J.A., Cooksley, G., 2013. *Multi-sensor advanced DInSAR monitoring of very slow landslides: the Tena Valley case study (Central Spanish Pyrenees)*. *Remote Sens. Environ.* 128, 31–43.
- Hung, W.C., Hwang, C., Chen, Y.A., Chang, C.P., Yen, J.Y., Hooper, A., Yang, C.Y., 2011. *Surface deformation from persistent scatterers SAR interferometry and fusion with leveling data: a case study over the Choushui River alluvial fan, Taiwan*. *Remote Sens. Environ.* 115, 957–967.
- Lauknes, T.R., Piyush Shanker, A., Dehls, J.F., Henderson, I.H.C., Larsen, Y., 2010. *Detailed rockslide mapping in northern Norway with small baseline and persistent scatterer interferometric SAR time series methods*. *Rem. Sens. Environ.* 114, 2097–2109.
- Lavecchia, G., Ferrarini, F., De Nardis, R., Visini, F., Barbano, M.S., 2007. *Active thrusting as possible seismogenic source in Sicily (Southern Italy): some insights from integrated structural-kinematic and seismological data*. *Tectonophysics* 445, 145–167.
- Lentini D F., Catalano D S., Carbone D S., 2000. *Carta geologica della Provincia di Messina: Servizio Geologico, S.E.L.C.A., Provincia Regionale di Messina, Assessorato Territorio, scale 1:50,000*.
- Liu, P., Li, Z., Hoey, T., Kincal, C., Zhang, J., Zeng, Q.M.J.P., 2013. *Using advanced InSAR time series techniques to monitor landslides movements in Badong of the Three Gorges region, China*. *Int. J. Appl. Earth Obs. Geoinf.* 21, 253–264.
- Meisina, C., Zucca, F., Notti, D., Colombo, A., Cucchi, G., Giannico, C., Bianchi, M., 2008. *Geological interpretation of PSInSAR data at regional scale*. *Sensors* 8 (11), 7469–7492.
- Mondini, A.C., Guzzetti, F., Reichenbach, P., Rossi, M., Cardinali, M., Ardizzone, F., 2011. *Semi-automatic recognition and mapping of rainfall induced shallow landslides using optical satellite images*. *Remote Sens. Environ.* 115, 1743–1757.
- Notti, D., García-Davalillo, J.C., Herrera, G., Cooksley, G., 2010. *Assessment of the performance of X-band satellite radar data for landslide mapping and monitoring: Upper Tena Valley case study*. *Nat. Haz. Earth Syst. Sci.* 10, 1865–1875.



- Raspini, F., Cigna, F., Moretti, S., 2012. [Multi-temporal mapping of land subsidence at basin scale exploiting persistent scatterer interferometry: case study of Gioia Tauro plain \(Italy\)](#). *J. Maps* 8 (4), 514–524.
- Righini, G., Pancioli, V., Casagli, N., 2012. [Updating landslide inventory maps using Persistent Scatterer Interferometry \(PSI\)](#). *Int. J. Remote Sens.* 33 (7), 2068–2096.
- Somma, R., Messina, A., Mazzoli, S., 2005. [Syn-orogenic extension in the Peloritani Alpine Thrust Belt \(NE Sicily, Italy\): evidence from the Ali unit](#). *Compt. Rend. Geosci.* 337, 861–871.
- Tomás, R., García-Barba, J., Cano, M., Sanabria, M.P., Ivorra, S., Duro, J., Herrera, G., 2012. [Subsidence damage assessment of a gothic church using Differential Interferometry and field data](#). *Struct. Health Monit.* 11, 751–762.